

Bottomonia screening masses from 2 + 1 flavor QCD

Peter Petreczky,^a Sayantan Sharma^{b,*} and Johannes Heinrich Weber^c

^a*Physics Department, Brookhaven National Laboratory,
Upton NY 11973, USA*

^b*The Institute of Mathematical Sciences, HBNI,
Chennai, 600113, India*

^c*Institut für Physik, Humboldt-Universität zu Berlin & IRIS Adlershof,
D-12489 Berlin, Germany*

E-mail: sayantans@imsc.res.in

The sequential melting of the bottomonium states is one of the important signals for the existence of a quark gluon plasma. The study of bottomonia spectral functions on the lattice is a difficult task for many reasons. Calculations based on NRQCD, that are commonly used for such purpose, are not applicable at high temperatures. In this work we propose a new method to study this problem by calculating the spatial screening masses of bottomonium states. We calculate the spatial meson correlators and extract the screening masses for mesons in different quantum channels using highly improved staggered quark (HISQ) action for bottom quarks and dynamical 2+1 flavor QCD HISQ gauge configurations. The typical lattices we choose are of size $N_s^3 \times N_\tau$ where $N_s = 4N_\tau$ and $N_\tau = 8, 10, 12$. We consider the temperature range $T = 300-1000$ MeV. We show that for $T > 500$ MeV the temperature dependence of the screening masses of the ground state bottomonia are compatible with the expectations based on uncorrelated quark anti-quark pairs.

*The 38th International Symposium on Lattice Field Theory, LATTICE2021 26th-30th July, 2021
Zoom/Gather@Massachusetts Institute of Technology*

*Speaker

1. Introduction

The dissolution of the bound state of heavy quarks called quarkonium has been suggested as one of the remarkable signals of the formation of a quark-gluon plasma in heavy-ion collisions [1]. Recent experimental results from CMS have given some tantalizing signals of the relative suppression of bottomonium $\Upsilon(2s)$ state compared to its ground state [2] and further experimental efforts are ongoing to understand charmonium suppression at RHIC and LHC. At the same time, recent phenomenological studies of the dynamics of quarkonia have produced many new insights about the widths and lifetimes of such states, see for example, Refs. [3, 4] for recent reviews.

In principle, the properties of quarkonium are all encoded in its spectral function defined in terms of the real-time correlation function of the appropriate hadron operator. At finite temperature, the peaks in the spectral function at frequencies equal to the masses of the bound states are expected to be broadened and shifted in the frequency domain, and eventually merge into the continua of quark-antiquark scattering states. However calculating the spectral functions non-perturbatively in a quantum field theory is immensely challenging. Within lattice QCD it is possible, in-principle, to calculate the quarkonium spectral functions through an analytic continuation of the Euclidean time correlation functions for that specific quantum number channel, calculated using lattice field theory techniques. However, the reconstruction of the spectral function from a discrete set of Euclidean correlator data is an ill-defined problem. A specific reconstruction method of the spectral functions using the maximum entropy method has been used extensively and the initial results on quarkonia spectral functions can be found in [5–10]. At higher temperatures, limited extent of the lattice along the temporal direction adds to the systematic difficulties in extracting the in-medium quarkonium functions [11, 12].

For bottomonium an additional systematic uncertainty in the lattice results arise due large bottom quark mass in the form of mass-dependent discretization errors. Attempts to circumvent this problem using non-relativistic QCD (NRQCD), have yielded several interesting insights on bottomonium properties [13–17]. Recent lattice studies within the NRQCD effective theory [18–23] have shown that ground states of bottomonium channels, $\Upsilon(1S)$ and $\eta_b(1S)$ can survive up to temperatures of 400 MeV, whereas significant disagreements exist over the fate of P -wave bottomonium in the quark-gluon plasma. Furthermore, since NRQCD is a long-distance effective theory which is defined only for not too small lattice spacings, we cannot study the high temperature regime as $T = 1/(aN_\tau)$ with N_τ being the temporal extent. We have thus proposed to study the problem of bottomonia melting using a new observable, the screening mass corresponding to different bottomonia channels in Ref. [24], the results of which we highlight in this talk.

2. Bottomonium screening correlation functions on the lattice

The spatial correlation functions can offer a different perspective on the problem of in-medium modification of mesons since these are in turn related to meson spectral functions at non-zero momenta through the relation,

$$G(z, T) = \int_0^\infty \frac{2d\omega}{\omega} \int_{-\infty}^\infty dp_z e^{ip_z z} \sigma(\omega, p_z, T). \quad (1)$$

At large distances the spatial meson correlation function decays exponentially, and this exponential decay is governed by the *screening mass*, extracted from the relation $G(z, T) \sim \exp(-M_{\text{scr}}(T) z)$. For well-defined bound state peaks in the meson spectral functions, the corresponding screening mass is simply the pole mass. When the quark and anti-quarks are eventually unbound at high temperatures, the screening mass is given by $2\sqrt{(\pi T)^2 + m_q^2}$, with m_q being the quark mass. Thus the temperature dependence of the meson screening masses can provide some valuable information about the melting of meson states. Moreover the spatial meson correlation functions can be calculated for large spatial separations between the quark and anti-quarks, therefore are more sensitive to in-medium modifications of meson states [25, 26].

We study the bottomonia screening masses on the lattice using the highly improved staggered quark (HISQ) discretization for the quarks. Not only does the choice of HISQ action minimize the taste-splitting for the light quark states, it also preserves the correct dispersion relation for heavy quarks [27]. Within the staggered fermion formalism the meson currents are defined as

$$J_M(\mathbf{x}) = \bar{q}(\mathbf{x})(\Gamma_D \times \Gamma_F)q(\mathbf{x}), \quad \mathbf{x} = (x, y, z, \tau), \quad (2)$$

where Γ_D, Γ_F are the Dirac gamma-matrices corresponding to the spin and the staggered tastes. We will consider only the case where $\Gamma_D = \Gamma_F = \Gamma$. This corresponds to local operators for the meson currents, which in terms of the staggered quark fields $\chi(\mathbf{x})$ and the phases $\tilde{\phi}(\mathbf{x})$ have a simple form $J_M(\mathbf{x}) = \tilde{\phi}(\mathbf{x})\bar{\chi}(\mathbf{x})\chi(\mathbf{x})$. Specific choices of the staggered phases correspond to mesonic excitations with different quantum numbers. Summing over the temporal and any two other spatial coordinates, we arrive at the expression of the screening correlator $C_M(z) = \sum_{x,y,\tau} \langle J_M(\mathbf{x})J_M(0) \rangle$. The staggered meson correlation function contains contributions from both parity states which correspond to the oscillating (O) and non-oscillating (NO) parts in the correlator. For the lowest energy states the screening correlation function for the mesons can be simply written as

$$C_M(z) = A_{NO} \cosh \left[M_{NO} \left(z - \frac{N_s}{2} \right) \right] - (-1)^z A_O \cosh \left[M_O + \left(z - \frac{N_s}{2} \right) \right].$$

For example, the NO part of the correlator for the staggered phase $\tilde{\phi} = -1$ correspond to the pseudo-scalar η_b channel whereas the corresponding oscillating part correspond to the scalar χ_{b0} excitation. For the quantum number assignments to different bottomonium states, see Ref. [24].

3. Numerical setup

We calculate the screening masses of the bottomonium states in QCD with 2 + 1 flavors of dynamical light and strange quarks and treat the bottom quarks in the quenched approximation. We have used the dynamical gauge configurations which were generated by the HotQCD collaboration [28, 29] using tree-level Symanzik improved gauge action and HISQ action for the quarks. The strange quark mass, m_s was chosen close to its physical value, while the light quark masses $m_l = m_s/20$ correspond to a Goldstone pion mass of 160 MeV in the continuum limit [28]. We performed our study on a wide temperature range between $2 - 7 T_c$, where the chiral crossover temperature $T_c = 156.5(1.5)$ MeV [30]. This was done in order to understand the entire thermal evolution of the bottomonium screening correlators. In order to estimate the cut-off dependence of

our results at each temperature, we considered three different temporal extents of $N_\tau = 8, 10, 12$ but the spatial extent fixed in each case to be $N_s = 4N_\tau$. With these choices of lattice spacings we have ensured that $m_b a \leq 1$ for the entire temperature range such that the lattice artifacts are sufficiently small in the bottomonium correlators.

The bottom quark mass in this entire range has been set to be $52.5m_s$, which is very close to its physical value. The details of the lattice parameters including the inverse of the bare lattice gauge coupling $\beta = 10/g_0^2$, quark masses, temperatures as well as the number of configurations used are mentioned in Table 1. The values of temperature were set using r_1 -scale where we have taken $r_1 = 0.3106(18)$ fm [31]. We have used point sources corresponding to both the bottom quark and its anti-particle in the meson correlators and performed two-state fits of the corresponding correlators using Eq. (3) in order to determine the bottomonium screening masses.

β	am_s	am_b	$N_\tau = 8$		$N_\tau = 10$		$N_\tau = 12$	
			T (MeV)	# confs	T (MeV)	# confs	T (MeV)	# confs
7.650	0.0192	1.01	-	-	-	-	349	220
7.825	0.0164	0.86	610	500	488	250	407	180
8.000	0.0140	0.74	710	500	568	500	473	180
8.200	0.0117	0.61	842	250	674	250	561	500
8.400	0.0098	0.52	998	240	798	250	665	500
8.570	0.0084	0.44	-	-	922	250	768	250
8.710	0.0074	0.39	-	-	-	-	864	250
8.850	0.0065	0.34	-	-	-	-	972	250

Table 1: The entire list of inverse bare gauge couplings, β , quark masses, temperature values and the corresponding number of gauge configurations (#confs) used in this study.

4. Results

We summarize here our main findings, for a more detailed discussion of our results for bottomonia screening masses we refer to our published work [24].

- At the lowest temperatures, the η_b screening mass is close to the zero temperature mass, while at high temperatures $T > 500$ MeV the screening mass increases linearly with temperature, signalling melting of η_b as shown in Fig. 1.
- Also seen in Fig. 1, the ratio $M_{\text{scr}}^{\text{PS}}/M_{\eta_b}$ shows a slow convergence to its corresponding values from NLO perturbation theory at $T > 500$ MeV, suggesting a gradual melting of η_b into a pair of correlated $b\bar{b}$ pairs.
- As evident from the left panel of Fig. 2 at the lowest two temperatures the difference between the vector and pseudo-scalar screening masses are consistent with the hyperfine splitting that exists between the $\Upsilon(1S)$ and $\eta_b(1S)$ states which is about 70 MeV [32]. This suggests that

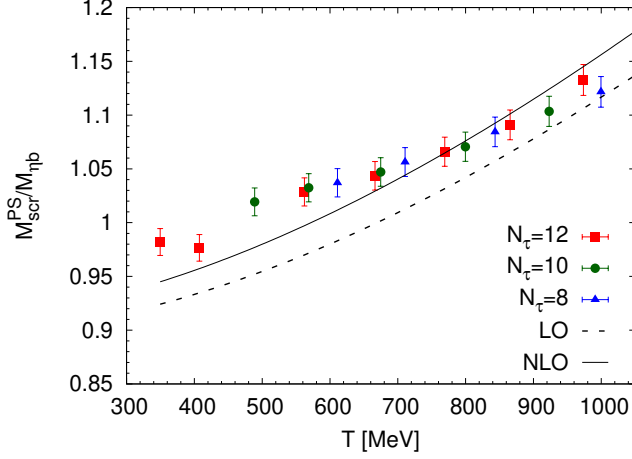


Figure 1: The pseudo-scalar screening mass normalized by the mass of $\eta_b(1S)$ meson at zero temperature, as function of the temperature obtained on lattices with $N_\tau = 8, 10$ and 12 . The solid line depicts the prediction for the screening mass at lowest order (LO) in perturbation theory, while the dashed line is the NLO prediction, taken from Ref. [24].

at these temperatures the $\eta_b(1S)$ and $\Upsilon(1S)$ exist as well defined bound states with little in-medium modifications.

- For $T > 450$ MeV the difference between vector and pseudo-scalar screening masses increases linearly with temperature as shown in the left panel of Fig. 2. Within perturbation theory at NLO in strong-coupling constant this difference is identically zero. One can understand this observation within a three dimensional effective theory of QCD. In this effective theory, a quark and anti-quark propagating along the z -direction, interact via a spin-dependent potential which is proportional to the temperature [33] giving a mass splitting of $0.3 T$ at $T > 900$ MeV.
- Since these spin-dependent interactions are inversely proportional to the quark mass, its effects in the mass splitting between vector and pseudo-scalar screening states is negligibly small for the bottom sector as compared to the light quark sector.
- Furthermore from the right panel of Fig. 2, the difference between the scalar and pseudo-scalar (or between the axial-vector and vector) screening masses agree with the differences between the $\chi_{b0}(1P)$ and $\eta_b(1S)$ ($\chi_{b1}(1P)$ and $\Upsilon(1S)$) masses reported in the Particle Data Group [32]. This again suggests that $\chi_{b0}(1P)$ and $\chi_{b1}(1P)$ states exist as confined states at $T = 350$ MeV with relatively small medium modifications. A large drop in this observable is seen for $350 < T < 600$ MeV, which approaches zero gradually owing to tiny effects of the bottom quark mass. Eventually in the regime when $T \gg m_b$, this difference should vanish.

5. Discussion on the possible systematics

- *Setting the bottom quark mass:* We have chosen the ratio of $m_b/m_s = 52.5$ which is close to its physical value. However the lines of constant physics for the strange quark mass have not

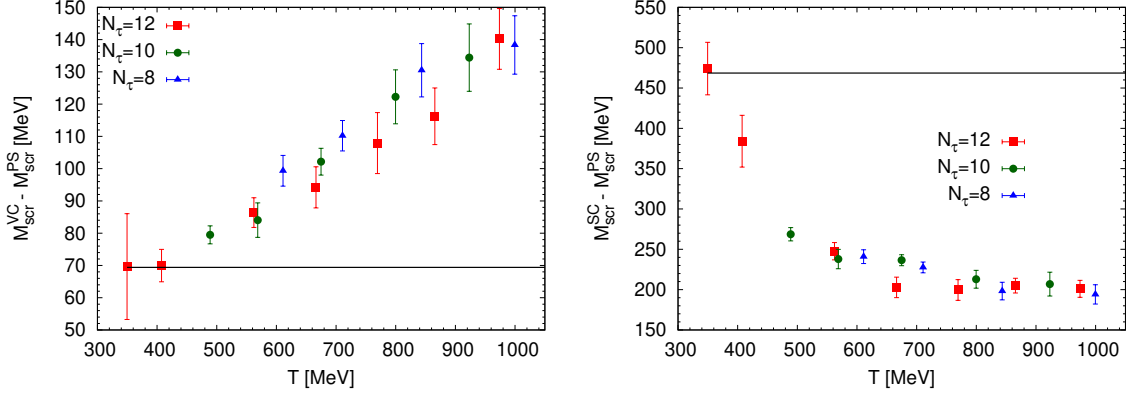


Figure 2: The left panel shows the difference between the vector and pseudo-scalar screening masses as function of the temperature obtained on lattices with $N_{\tau} = 8, 10$ and 12 , from Ref. [24]. The solid line corresponds to the difference between the $\Upsilon(1S)$ mass and the $\eta_b(1S)$ mass reported in the Particle Data Group. The right panel shows the difference between the scalar and pseudo-scalar screening masses as function of the temperature obtained on lattices with $N_{\tau} = 8, 10$ and 12 , from Ref. [24]. The solid line corresponds to the difference between the $\eta_b(1S)$ and the $\chi_{b0}(1P)$ mass, from Particle Data Group.

been fixed very precisely for the entire temperature range we have studied [28]. Hence it is not possible to simply set the η_b mass (used in the ratio shown in Fig. 1) to its experimentally measured value. From the estimated dependence of the η_b mass on the b quark mass for the HISQ action [34], it turns out that the η_b mass is larger than the PDG value by 4% and 9.8% for $\beta = 7.596$ and $\beta = 8.4$ respectively. At still higher values of β where no previous measurements exist, we assume that the η_b mass is 9.8% larger than the experimentally measured value.

- *Sources of systematic errors in the data:* We did not calculate the zero temperature mass for η_b explicitly for all the lattice spacings we have studied but estimated them based on interpolation, thus we have assigned a systematic error of 1% to the zero temperature mass for η_b . Moreover the errors in the scale setting of a/r_1 as well as the error in measuring r_1 in physical units also adds to the systematic error. All these error estimates were added in quadrature and combined together with the statistical errors, in order to estimate the error bars in the data points of Fig. 1. In the screening mass differences shown in Fig. 2, the effects due to the small deviation of bottom quark mass from its physical value is tiny. Thus in estimating the errors for these observables, we have simply added the errors in the determination of lattice spacings and the statistical errors in quadrature.
- *Cut-off effects in the data:* Quite surprisingly and assuredly we do not observe significant cut-off dependence in the screening mass results in the bottomonium sector, since the data agrees within errors for all three different N_{τ} values in all the plots.

6. Summary and outlook

We have presented here the main findings of a first comprehensive study about the temperature dependence of the bottomonium screening masses on the lattice using a relativistic action (HISQ)

for the bottom quarks. The observables we have proposed are rather insensitive to finite lattice cut-off effects, allowing us to make some very robust predictions [24]. To summarize our main findings,

- Our estimate of η_b melting temperature is about 450 MeV. This is consistent with the results from NRQCD based studies [18, 19, 21–23] as well as with the results from potential models with a screened complex potential [35, 36].
- We observe a linear dependence of the η_b mass with temperature for $T > 500$ MeV. For charmonium the linear increase with the temperature for η_c screening mass is seen already at $T > 250$ MeV [26] showing a clear mass-hierarchy in the melting of quarkonia.
- The $1P$ -bottomonia melt already at a comparatively lower temperature ~ 350 MeV, thus showing that the ground state bottomonia are more robust against in-medium modifications compared to their excited states.

Acknowledgments: PP was supported by U.S. Department of Energy under Contract No. DE-SC0012704. JHW work was supported by U.S. Department of Energy, Office of Science, Office of Nuclear Physics and Office of Advanced Scientific Computing Research within the framework of Scientific Discovery through Advance Computing (SciDAC) award Computing the Properties of Matter with Leadership Computing Resources, and by the Deutsche Forschungsgemeinschaft (DFG, German Research Foundation) - Projektnummer 417533893/GRK2575 “Rethinking Quantum Field Theory”. SS gratefully acknowledges financial support from the Department of Science and Technology, Govt. of India, through a Ramanujan Fellowship.

References

- [1] T. Matsui and H. Satz, *J/ψ Suppression by Quark-Gluon Plasma Formation*, *Phys. Lett.* **B178** (1986) 416.
- [2] CMS collaboration, *Suppression of $\Upsilon(1S)$, $\Upsilon(2S)$ and $\Upsilon(3S)$ production in PbPb collisions at $\sqrt{s_{NN}} = 2.76$ TeV*, *Phys. Lett. B* **770** (2017) 357 [1611.01510].
- [3] G. Aarts et al., *Heavy-flavor production and medium properties in high-energy nuclear collisions - What next?*, *Eur. Phys. J.* **A53** (2017) 93 [1612.08032].
- [4] A. Mocsy, P. Petreczky and M. Strickland, *Quarkonia in the Quark Gluon Plasma*, *Int. J. Mod. Phys.* **A28** (2013) 1340012 [1302.2180].
- [5] Y. Nakahara, M. Asakawa and T. Hatsuda, *Hadronic spectral functions in lattice QCD*, *Phys. Rev.* **D60** (1999) 091503 [hep-lat/9905034].
- [6] M. Asakawa and T. Hatsuda, *J/psi and eta(c) in the deconfined plasma from lattice QCD*, *Phys. Rev. Lett.* **92** (2004) 012001 [hep-lat/0308034].
- [7] F. Karsch, S. Datta, E. Laermann, P. Petreczky, S. Stickan and I. Wetzorke, *Hadron correlators, spectral functions and thermal dilepton rates from lattice QCD*, *Nucl. Phys.* **A715** (2003) 701 [hep-ph/0209028].

- [8] T. Umeda, K. Nomura and H. Matsufuru, *Charmonium at finite temperature in quenched lattice QCD*, *Eur. Phys. J.* **C39S1** (2005) 9 [[hep-lat/0211003](#)].
- [9] S. Datta, F. Karsch, P. Petreczky and I. Wetzorke, *Behavior of charmonium systems after deconfinement*, *Phys. Rev.* **D69** (2004) 094507 [[hep-lat/0312037](#)].
- [10] A. Jakovac, P. Petreczky, K. Petrov and A. Velytsky, *Quarkonium correlators and spectral functions at zero and finite temperature*, *Phys. Rev.* **D75** (2007) 014506 [[hep-lat/0611017](#)].
- [11] A. Mocsy and P. Petreczky, *Can quarkonia survive deconfinement?*, *Phys. Rev.* **D77** (2008) 014501 [[0705.2559](#)].
- [12] P. Petreczky, *On temperature dependence of quarkonium correlators*, *Eur. Phys. J.* **C62** (2009) 85 [[0810.0258](#)].
- [13] G.P. Lepage, L. Magnea, C. Nakhleh, U. Magnea and K. Hornbostel, *Improved nonrelativistic QCD for heavy quark physics*, *Phys. Rev.* **D46** (1992) 4052 [[hep-lat/9205007](#)].
- [14] C.T.H. Davies, K. Hornbostel, A. Langnau, G.P. Lepage, A. Lidsey, J. Shigemitsu et al., *Precision Upsilon spectroscopy from nonrelativistic lattice QCD*, *Phys. Rev.* **D50** (1994) 6963 [[hep-lat/9406017](#)].
- [15] S. Meinel, *Bottomonium spectrum at order v^6 from domain-wall lattice QCD: Precise results for hyperfine splittings*, *Phys. Rev.* **D82** (2010) 114502 [[1007.3966](#)].
- [16] T.C. Hammant, A.G. Hart, G.M. von Hippel, R.R. Horgan and C.J. Monahan, *Radiative improvement of the lattice NRQCD action using the background field method and application to the hyperfine splitting of quarkonium states*, *Phys. Rev. Lett.* **107** (2011) 112002 [[1105.5309](#)].
- [17] HPQCD collaboration, *The Upsilon spectrum and the determination of the lattice spacing from lattice QCD including charm quarks in the sea*, *Phys. Rev.* **D85** (2012) 054509 [[1110.6887](#)].
- [18] G. Aarts, S. Kim, M.P. Lombardo, M.B. Oktay, S.M. Ryan, D.K. Sinclair et al., *Bottomonium above deconfinement in lattice nonrelativistic QCD*, *Phys. Rev. Lett.* **106** (2011) 061602 [[1010.3725](#)].
- [19] G. Aarts, C. Allton, T. Harris, S. Kim, M.P. Lombardo, S.M. Ryan et al., *The bottomonium spectrum at finite temperature from $N_f = 2 + 1$ lattice QCD*, *JHEP* **07** (2014) 097 [[1402.6210](#)].
- [20] S. Kim, P. Petreczky and A. Rothkopf, *Lattice NRQCD study of S- and P-wave bottomonium states in a thermal medium with $N_f = 2 + 1$ light flavors*, *Phys. Rev.* **D91** (2015) 054511 [[1409.3630](#)].
- [21] S. Kim, P. Petreczky and A. Rothkopf, *Quarkonium in-medium properties from realistic lattice NRQCD*, *JHEP* **11** (2018) 088 [[1808.08781](#)].

- [22] R. Larsen, S. Meinel, S. Mukherjee and P. Petreczky, *Thermal broadening of bottomonia: Lattice nonrelativistic QCD with extended operators*, *Phys. Rev. D* **100** (2019) 074506 [1908.08437].
- [23] R. Larsen, S. Meinel, S. Mukherjee and P. Petreczky, *Excited bottomonia in quark-gluon plasma from lattice QCD*, *Phys. Lett. B* **800** (2020) 135119 [1910.07374].
- [24] P. Petreczky, S. Sharma and J.H. Weber, *Bottomonium melting from screening correlators at high temperature*, *Phys. Rev. D* **104** (2021) 054511 [2107.11368].
- [25] F. Karsch, E. Laermann, S. Mukherjee and P. Petreczky, *Signatures of charmonium modification in spatial correlation functions*, *Phys. Rev. D* **85** (2012) 114501 [1203.3770].
- [26] A. Bazavov, F. Karsch, Y. Maezawa, S. Mukherjee and P. Petreczky, *In-medium modifications of open and hidden strange-charm mesons from spatial correlation functions*, *Phys. Rev. D* **91** (2015) 054503 [1411.3018].
- [27] HPQCD COLLABORATION, UKQCD COLLABORATION collaboration, *Highly improved staggered quarks on the lattice, with applications to charm physics*, *Phys.Rev.* **D75** (2007) 054502 [hep-lat/0610092].
- [28] HOTQCD collaboration, *Equation of state in $(2+1)$ -flavor QCD*, *Phys. Rev.* **D90** (2014) 094503 [1407.6387].
- [29] H.T. Ding, S. Mukherjee, H. Ohno, P. Petreczky and H.P. Schadler, *Diagonal and off-diagonal quark number susceptibilities at high temperatures*, *Phys. Rev. D* **92** (2015) 074043 [1507.06637].
- [30] HOTQCD collaboration, *Chiral crossover in QCD at zero and non-zero chemical potentials*, *Phys. Lett. B* **795** (2019) 15 [1812.08235].
- [31] MILC collaboration, *Results for light pseudoscalar mesons*, *PoS LATTICE2010* (2010) 074 [1012.0868].
- [32] PARTICLE DATA GROUP collaboration, *Review of Particle Physics*, *Phys. Rev. D* **98** (2018) 030001.
- [33] V. Koch, E.V. Shuryak, G.E. Brown and A.D. Jackson, *The Propagation of quarks in the spatial direction in hot QCD*, *Phys. Rev. D* **46** (1992) 3169 [hep-ph/9204236].
- [34] P. Petreczky and J.H. Weber, *Strong coupling constant and heavy quark masses in $(2+1)$ -flavor QCD*, *Phys. Rev. D* **100** (2019) 034519 [1901.06424].
- [35] P. Petreczky, C. Miao and A. Mocsy, *Quarkonium spectral functions with complex potential*, *Nucl. Phys.* **A855** (2011) 125 [1012.4433].
- [36] Y. Burnier, O. Kaczmarek and A. Rothkopf, *Quarkonium at finite temperature: Towards realistic phenomenology from first principles*, *JHEP* **12** (2015) 101 [1509.07366].